引用格式：XU Xin, YE Huichun, JIN Xueying, et al. Influence of High-order Dispersion on Turing Patterns in Microresonators[J]. Acta Photonica Sinica, 2022, 51(11):1113001
徐昕,叶回春,金雪莹,等.光学微腔中高阶色散对图灵环光场的影响[J].光子学报,2022,51(11):1113001

光学微腔中高阶色散对图灵环光场的影响

徐昕[1],叶回春[2],金雪莹[1],高浩然[1],陈东[1],陆洋[3],于连栋[3]
(1 合肥工业大学 仪器科学与光电工程学院测量理论与精密仪器安徽省重点实验室, 合肥 230009)
(2 中国科学技术大学 精密机械与精密仪器系,合肥 230027)
(3 中国石油大学(华东) 控制科学与工程学院,山东 青岛 266555)

摘　要:光学微腔中高阶色散会对腔内的图灵环光场产生重要的影响,基于Lugiato-Lefever方程,采用分步傅立叶法对方程求解,分析光场在腔内的演化过程。研究发现,微腔中的奇次高阶色散会导致图灵环光场以恒定的速度发生时间漂移,色散系数的正负会导致漂移方向不同,且色散值越大,漂移速度也越大;偶次高阶色散不会对腔中的图灵光场产生影响。此外,高阶色散会引起图灵光场中的高阶模式产生较强的色散波。

关键词:超快光学;光学微腔;图灵环;高阶色散,色散波
中图分类号:O437　　**文献标识码**:A　　**doi**:10.3788/gzxb20225111.1113001

0　引言

基于光学微腔的光频梳技术因其结构紧凑、集成度高、功耗低等优点,得到了广泛的应用[1,2]。由于光学微腔对光场的束缚,可在腔内产生极高的功率密度,进而由四波混频效应产生光频梳[3]。当光场经过混沌后,可在腔内演化成光频梳,光谱中相邻两个模式之间的频率间隔是一个或者多个自由光谱范围(Free Spectral Range, FSR)。其中频率间隔是一个FSR的情况是孤子光场[4-6]。但是当腔内的调制不稳定性(Modulation Instability, MI)起主要作用时,可产生自发的图灵环光场[7],和孤子光场相比,图灵环在频域上拥有更大的梳齿频率间隔[8-9]。图灵环光场凭借其良好的光谱特性和抗干扰性,被应用于大容量通信[10]、片上光场压缩等领域[11]。研究者利用Lugiato-Lefever方程(Lugiato-Lefever Equation,LLE)对图灵环光场的产生机制展开了研究,并且已经在实验中产生了图灵环光场[12-13]。但是在已有的研究中,光学微腔的高阶色散往往被忽略。有研究表明,微腔中的高阶色散会对腔内孤子以及暗孤子光场产生一定影响[14],并且宽带频率梳的光谱可以通过高阶色散的取值来调节[15]。然而,目前还未见关于高阶色散对图灵环光场影响的研究,因此本文以LLE为理论模型,研究了光学微腔中高阶色散对图灵环光场的影响,并分析了高阶色散作用下的模式色散情况。

1　理论模型和分析

光学微腔中的光场演化过程可以用归一化的LLE来描述[16-18],即

$$\frac{\partial\psi}{\partial\tau}=-(1+\mathrm{i}\alpha)\psi+\left|\psi\right|^2\psi-\sum_{n=2}^{N}(-\mathrm{i})^{n+1}\frac{\beta_n}{n!}\frac{\partial^n\psi}{\partial\theta^n}+F \tag{1}$$

式中,ψ表示光场分布,它是慢时间τ和方位角θ的函数,$\theta\in[-\pi,\pi]$;α是微腔谐振模式和泵浦模式之间的频

基金项目:国家自然科学基金(Nos. 52175503, 52005147),国家重点研发计划(No. 2019YFE0107400)
第一作者:徐昕(1986—),女,讲师,博士,主要研究方向为超快光纤技术及应用。Email:xuxin@hfut.edu.cn
通讯作者:金雪莹(1991—),女,讲师,博士,主要研究方向为微腔光频梳及精密测量。Email:xyjin007@hfut.edu.cn
于连栋(1971—),男,教授,博士,主要研究方向为超快激光精密测试。Email:liandongyu@upc.edu.cn
收稿日期:2022-04-27;**录用日期**:2022-06-06

率失谐，β_n表示泵浦模数对应的n阶色散系数，N表示微腔内总的色散阶数，F表示泵浦强度。本文只讨论高阶色散对光场的影响，因此忽略了微腔中的自陡峭和拉曼效应。之前的研究表明，在负色散的光学微腔中，图灵环源自于腔内的噪声光场[13]。当泵浦强度F满足阈值条件$F_{th}^2=1+(1-\alpha)^2$时，图灵环光场即可在微腔内产生。

腔内的总能量E、时间位置参数T_p和频率漂移参数Ω_p可分别表示为

$$E=\int_{-\pi}^{\pi}|\psi|^2\mathrm{d}\theta \tag{2}$$

$$T_p=\frac{1}{E}\int_{-\pi}^{\pi}\theta|\psi|^2\mathrm{d}\theta \tag{3}$$

$$\Omega_p=\frac{\mathrm{i}}{2E}\int_{-\pi}^{\pi}\left(\psi^*\frac{\partial\psi}{\partial\theta}-\psi\frac{\partial\psi^*}{\partial\theta}\right)\mathrm{d}\theta \tag{4}$$

当光场分布ψ稳定时，腔内的色散和非线性效应、损耗和增益达到平衡，此时的光场能量E满足条件

$$\frac{\mathrm{d}E}{\mathrm{d}\tau}=0 \tag{5}$$

此外，频率的漂移主要是由拉曼效应引起，因为拉曼效应被忽略，所以频率漂移参数Ω_p满足条件

$$\frac{\mathrm{d}\Omega_p}{\mathrm{d}\tau}=0 \tag{6}$$

时间位置T_p随时间的变化关系为[14]

$$\frac{\mathrm{d}T_p}{\mathrm{d}\tau}=-\frac{1}{E}\sum_{n\geqslant1}\int_{-\pi}^{\pi}\frac{\beta_{2n+1}}{(2n)!}\left|\frac{\partial^n E}{\partial\theta^n}\right|^2\mathrm{d}\theta+\frac{\mathrm{i}}{E}\sum_{n\geqslant1}\int_{-\pi}^{\pi}\frac{\beta_{2n}}{(2n)!}n\left(\frac{\partial^n E}{\partial\theta^n}\frac{\partial^{n-1}E^*}{\partial\theta^{n-1}}-\frac{\partial^n E^*}{\partial\theta^n}\frac{\partial^{n-1}E}{\partial\theta^{n-1}}\right)\mathrm{d}\theta \tag{7}$$

考虑傅立叶变换中时域和频域的对应关系

$$F\left[\frac{\partial^n E(\tau,\theta)}{\partial\theta^n}\right]=(-\mathrm{i}\omega)^n\tilde{E}(\tau,\omega) \tag{8}$$

式中，$F[\cdot]$表示傅立叶变化。利用式(8)，式(7)可以被简化为

$$\frac{\mathrm{d}T_p}{\mathrm{d}\tau}=-\frac{1}{E}\sum_{n\geqslant1}\int_{-\pi}^{\pi}\frac{\beta_{2n+1}}{(2n)!}\left|\frac{\partial^n E}{\partial\theta^n}\right|^2\mathrm{d}\theta \tag{9}$$

根据式(9)，分别考虑高阶色散中的β_3和β_5，位置漂移可以分别写为

$$\left(\frac{\mathrm{d}T_p}{\mathrm{d}\tau}\right)_3=-\frac{1}{E}\int_{-\pi}^{\pi}\frac{\beta_3}{2}\left|\frac{\partial E}{\partial\theta}\right|^2\mathrm{d}\theta \tag{10}$$

$$\left(\frac{\mathrm{d}T_p}{\mathrm{d}\tau}\right)_5=-\frac{1}{E}\int_{-\pi}^{\pi}\frac{\beta_5}{24}\left|\frac{\partial^2 E}{\partial\theta^2}\right|^2\mathrm{d}\theta \tag{11}$$

可以看到，只有奇次的高阶色散可以引起光场位置的漂移，并且色散系数越大，漂移速度也越快。

为进一步研究高阶色散对图灵环光场的影响，利用广泛使用的分步傅立叶法求解LLE，分析微腔内光场的动态变化过程。依据图灵环光场的产生条件，假设腔内的初始光场为微弱的随机噪声，进行相应的理论计算和分析。

2 高阶色散对图灵环光场的影响

在式(1)中，设置参数$\alpha=1.5$，$F=1.14$。分析中高阶色散被忽略，仅考虑微腔的二阶色散，光场分布的演化过程如图1(a)所示，腔内最终形成了6个在空间上等间距分布的脉冲，即典型的图灵环光场。当更高阶的三阶、四阶和五阶色散分别被考虑后，光场演化的结果如图1(b)～(d)所示，其中脉冲数量均保持不变，但是在考虑三阶和五阶色散的情况下，脉冲位置随时间发生变化。说明奇次高阶色散会引起图灵环光场的位置漂移。由于五阶色散系数的值较小，因此由五阶色散引起的光场漂移作用相对较弱，漂移的速度也相对较慢。需要说明的是，为了能够表示出光场的漂移，在图1(d)中，扩大了纵坐标时间轴的取值范围。另一方面，考虑偶次高阶色散对图灵环光场的影响，结果如图1(c)所示，在初始阶段，腔内光场在各种作用下没有

达到稳定状态，图灵环脉冲有微小的变化，当光场达到稳定后，脉冲的位置和形状保持不变。因此，在图1(c)所示的条件下，偶次高阶色散不会导致光场的漂移，光场位置没有发生变化。这一数值计算结果和第1节的理论分析结果相一致。

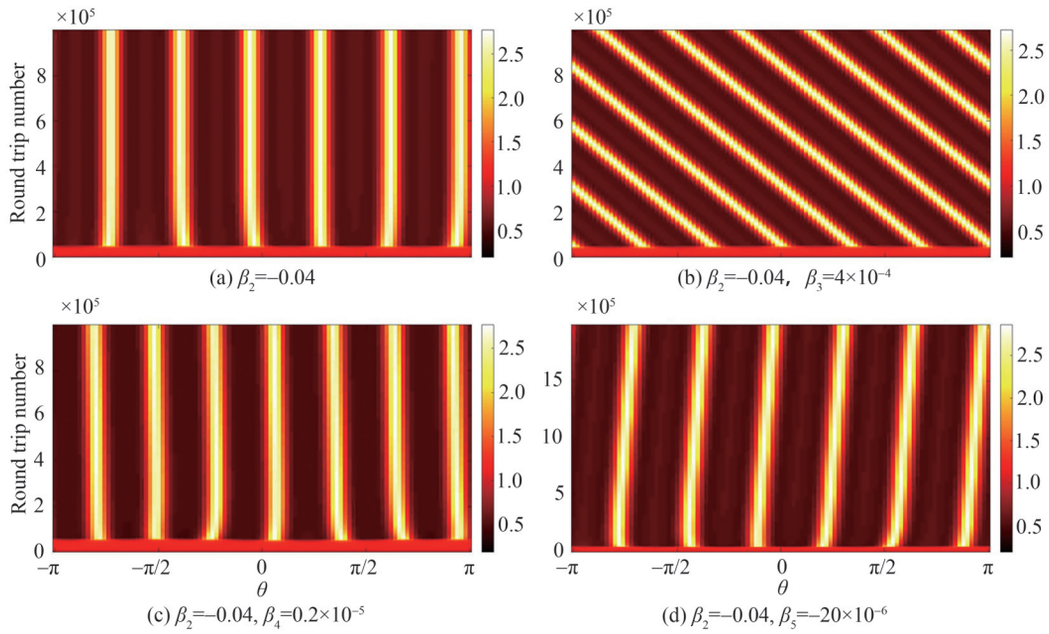

图1　不同高阶色散条件下图灵环光场的演化

Fig.1　Evolution of turing patterns with various higher-order dispersion parameters

此外，还研究了色散系数大小对光场漂移速度的影响。由于三阶色散对光场漂移的影响较为明显，因此只以三阶色散为例，其余参数设置和图1一样。图2(a)～(c)是三阶色散β_3取不同值时图灵环的演化情况。图2(a)中光场的漂移方向和图2(b)和(c)不同，是因为图2(a)中β_3的符号和图2(b)、(c)中的相反。因此，色散系数的正负号会影响到图灵环光场的漂移方向，但不会改变光场中的脉冲个数。将图2(a)中光场的漂移速度定义为正值，图2(b)和(c)的漂移速度为负值，β_3取不同值时的漂移速度曲线如图2(d)所示，随

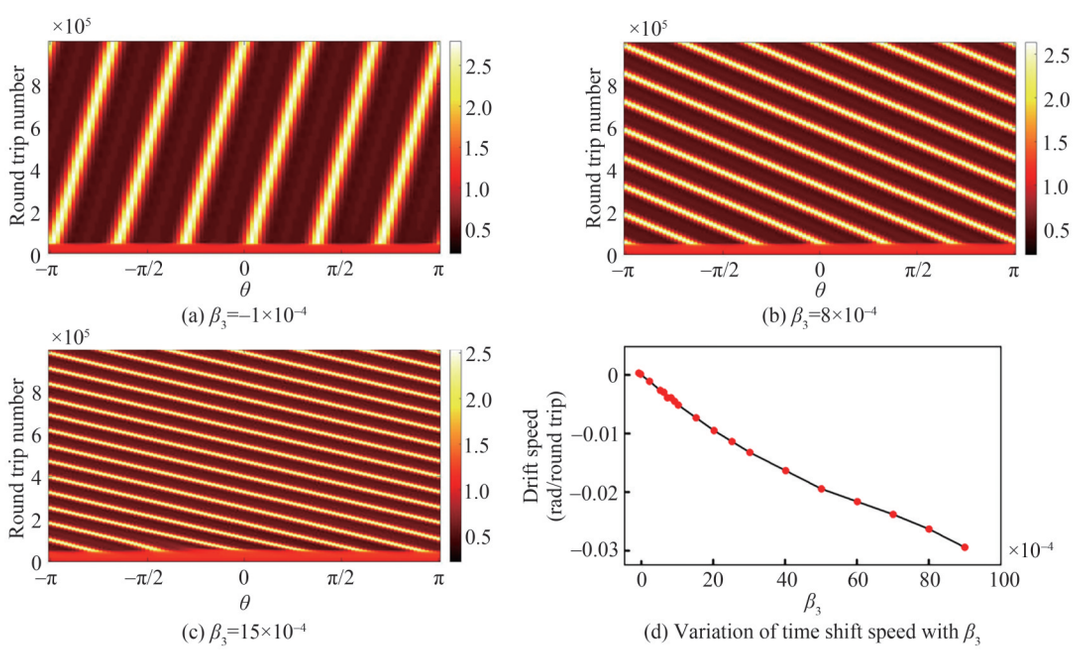

图2　β_3取不同值时图灵环光场的演化

Fig.2　Evolution of turing patterns with different β_3

着β_3值的增加，光场漂移速度的绝对值也增长，和式(10)的理论分析结果一致。

在光微腔中，当初始光场为高斯脉冲时，可以产生另一种多脉冲形式的光场分布。在图3(a)中，假设初始光场为$\psi_0=0.5+\exp[-(\theta/0.55)^2]$，失谐参数$\alpha=2.5$，泵浦参数$F=1.76$。在这种情况下，频率失谐在光场变化中起到主要作用，4个脉冲形式的光场在腔内产生，由于三阶色散的作用，这样一种多脉冲形式的光场也同样在腔内发生漂移。此外，高阶色散也会对光谱产生影响。根据色散辐射理论[19, 20]，色散波的频率可描述为

$$D(m)=\frac{\beta_3}{6}m^3-Vm\pm\sqrt{\left(\frac{\beta_2}{2}m^2+\frac{\beta_4}{24}m^4+2P-\alpha\right)^2-P_0^2} \tag{12}$$

式中，m表示模式数；V表示光场在腔内循环一周的位置漂移大小；P表示泵浦功率，和式(1)中的泵浦参数F值有关；P_0表示光场的背景功率。多脉冲光场对应的光谱以及色散波曲线如图3(b)所示，光谱在梳状谱的基础上受到了明显的调制。光谱和色散波曲线的位置关系表明，色散波曲线的零点位置对应光谱中的次峰值。保持三阶色散值不变，当失谐参数进一步增大时，多脉冲形式的光场演化成另一种形式的图灵环光场，如图3(c)所示，光场中包含了19个等间距的脉冲，因此其光谱相邻两个峰值间也有19个模式间隔，光谱次峰值的位置同样对应图3(d)中的色散波曲线的零点位置。需要说明的是，为了方便找到色散波曲线中的零点位置，在图中给出其绝对值曲线。结果表明，三阶色散可以引起图灵环光场和多脉冲光场的漂移，且色散波曲线零点的位置对应光场光谱次峰值的位置，意味着在考虑三阶色散的情况下，光学微腔中受激产生最强的新模式色散值是0。

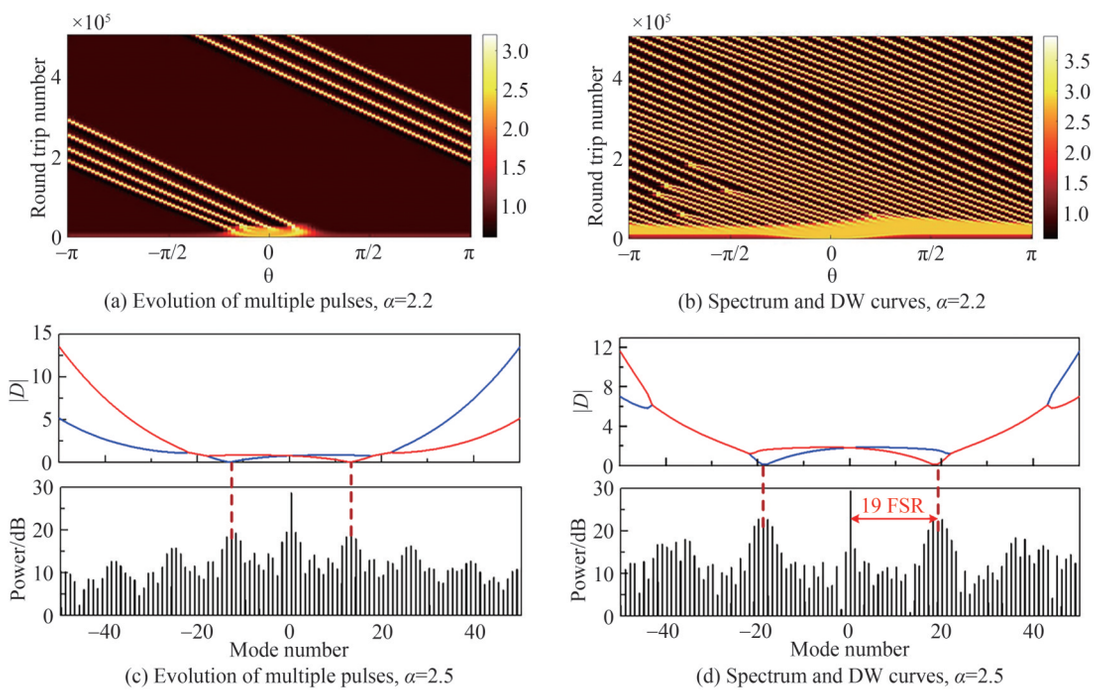

图3 腔内损耗对光场演化，色散波曲线及光谱的影响

Fig.3 Influence of microresonator loss on optical field evolutions, dispersion wave curves and spectra

研究了三阶色散对色散波曲线的影响。在图2的基础上绘制了β_3取不同值时的色散波曲线，如图4所示。在图3中可以看到，两条色散波曲线是对称关系，为了简便，图4中只给出其中一条色散波曲线，即式(12)中取正号的情况。由于β_3值的增加仅影响光场的漂移速度，而不改变光场的脉冲个数，因此色散波曲线的零点位置固定不变。在图4中，β_3的增加会导致色散波曲线斜率的增加，意味着高阶色散会引起图灵环光场中高阶模式的色散波增强，但是对其中的低阶模式几乎没有影响。低阶模式下，色散波强度几乎为0。

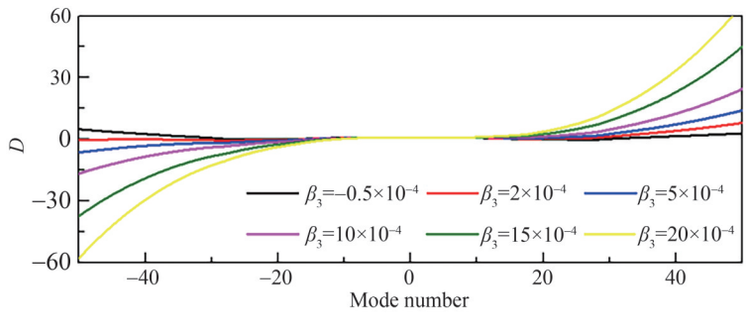

图4　β_3取不同值时的色散波曲线

Fig.4　Dispersive wave curves with different β_3

3　结论

本文以归一化的LLE为理论模型，分析了高阶色散对光学微腔内的图灵环光场。理论分析和数值计算结果均表明，奇次高阶色散会引起腔内图灵环光场以恒定速度漂移，而偶次高阶色散则不会对腔内光场产生影响。奇次高阶色散不仅直接关系到光场漂移的方向，还会影响漂移速度。以三阶色散为例，三阶色散值的正负对应着不同的光场漂移方向，其值越大，图灵环光场的漂移也越快。此外，在考虑高阶色散的情况下，研究了表征光谱性质的图灵环光场色散波曲线。色散波曲线中，零点的位置对应了光谱中次峰值的位置。高阶色散还会加强图灵环中高阶模式色散波的大小。理论分析结果对研究高阶色散不可忽略的光学微腔中的图灵环光场具有一定意义。

参考文献

[1] JOHNSON A R, OKAWACHI Y, LEVY J S, et al. Chip-based frequency combs with sub-100 GHz repetition rates[J]. Optics Letters, 2012, 37(5): 875-877.

[2] OKAWACHI Y, SAHA K, LEVY J S, et al. Octave-spanning frequency comb generation in a silicon nitride chip[J]. Optics Letters, 2011, 36(17):3398-3400.

[3] GRUDININ I S, YU N, MALEKI L. Generation of optical frequency combs with a CaF_2 resonator[J]. Optics Letters, 2009, 34(7):878-880.

[4] YI X, YANG Q F, ZHANG X Y, et al. Single-mode dispersive waves and soliton microcomb dynamics[J]. Nature Communications, 2017, 8: 14869.

[5] SLAVCHEVA G, GORBACH A V, PIMENOV A. Coupled spatial multi-mode solitons in microcavity wires[J]. Physical Review B, 2016, 94:245432.

[6] RAJA A S, VOLOSHIN A S, GUO H, et al. Electrically pumped photonic integrated soliton microcomb[J]. Nature Communications, 2019, 10:680.

[7] FATOME J, KIBLER B, LEO F, et al. Polarization modulation instability in a nonlinear fiber Kerr resonator[J]. Optics Letters, 2020, 45(18): 5069-5072.

[8] COILLET A, BALAKIREVA I, HENRIET R, et al. Azimuthal turing patterns, bright and dark cavity solitons in Kerr combs generated with whispering-gallery-mode resonators[J]. IEEE Photonics Journal, 2013, 5(4):6100409.

[9] COILLET A, CHEMBO Y K. On the robustness of phase locking in Kerr optical frequency combs[J]. Optics Letters, 2014, 39(6):1529-1532.

[10] PFEIFLE J, COILLET A, HENRIET R, et al. Optimally coherent Kerr combs generated with crystalline whispering gallery mode resonators for ultrahigh capacity fiber communications[J]. Physical Review Letters, 2015, 114:093902.

[11] DUTT A, LUKE K, MANIPATRUNI S, et al. On-chip optical squeezing[J]. Physical Review Applied, 2015, 3: 044005.

[12] BAO H L, OLIVIERI L, ROWLEY M, et al. Turing patterns in a fiber laser with a nested microresonator: robust and controllable microcomb generation [J]. Physical Review Research, 2020, 2:023395.

[13] GODEY C, BALAKIREVA I V, COILLET A, et al. Stability analysis of the spatiotemporal Lugiato-Lefever model for Kerr optical frequency combs in the anomalous and normal dispersion regimes[J]. Physical Review A, 2014, 89:063814.

[14] LIU M L, WANG L R, SUN Q B, et al. Influences of high-order dispersion on temporal and spectral properties of microcavity solitons[J]. Optics Express, 2018, 26(13):16477-16487.

[15] WANG S F, GUO H R, BAI X K, et al. Broadband Kerr frequency combs and intracavity soliton dynamics influenced by high-order cavity dispersion [J]. Optics Letters, 2014, 39(10):2880-2883.

[16] PARRA-RIVAS P, KNOBLOCH E, GOMILA D, et al. Dark solitons in the Lugiato-Lefever equation with normal dispersion[J]. Physical Review A, 2013, 93:063839.
[17] CHEMBO Y K, MENYUK C R. Spatiotemporal Lugiato-Lefever formalism for Kerr-comb generation in whispering-gallery-mode resonators[J]. Physical Review A, 2013, 87:053852.
[18] COEN S, RANDLE H G, SYLVESTRE T, et al. Modeling of octave-spanning Kerr frequency combs using a generalized mean-field Lugiato-Lefever model[J]. Optics Letters, 2013, 38(1):37-39.
[19] MILIÁN C, SKRYABIN D V. Soliton families and resonant radiation in a micro-ring resonator near zero group velocity dispersion[J]. Optics Express, 2014, 22(3):3732-3739.
[20] MALAGUTI S, CONFORTI M, TRILLO. Dispersive radiation induced by shock waves in passive resonators[J]. Optics Letters, 2014, 39(19):5626-5629.

Influence of High-order Dispersion on Turing Patterns in Microresonators

XU Xin[1], YE Huichun[2], JIN Xueying[1], GAO Haoran[1], CHEN Dong[1], LU Yang[3], YU Liandong[3]

(1 *Anhui Province Key Laboratory of Measuring Theory and Precision Instrument, School of Instrument Science and Optoelectronics Engineering, Hefei University of Technology, Hefei* 230009, *China*)

(2 *Department of Precision Machinery and Precision Instrumentation, University of Science and Technology of China, Hefei* 230027, *China*)

(3 *College of Control Science and Engineering, China University of Petroleum (UPC), Qingdao, Shandong* 266555, *China*)

Abstract: Microresonator-based optical frequency combs have attracted extensive interest due to their compactness, flexibility, low power consumption, and compatibility with complementary metal-oxide-semiconductor integration. When modulation instability dominates in nonlinear microresonators, a particular field of dissipative Turing patterns is demonstrated. Turing patterns exhibit wider frequency comb intervals than a soliton field in the spectral domain. Owing to their robustness against perturbations and optimal spectral purity, Turing patterns provide a creative platform for high-capacity communication, on-chip optical squeezing, and other applications.

At present, the effect of high order dispersion on Turing patterns is generally ignored. However, this effect is particularly important for microresonators with a large amount of high order dispersion. Therefore, the influence of high order dispersion on Turing patterns is investigated in this study. The step-Fourier is used to solve the theoretical model of Lugiato-Lefever Equation, the evolutions of the field inside the microresonators are investigated, and the influences of higher order dispersion on Turing ring optical field are also analyzed. The theoretical analysis and numerical calculation prove that the third-order dispersion coefficient β_3 causes a time shift in Turing patterns at a uniform speed. The fifth-order dispersion coefficient β_5, which is smaller than the third-order dispersion coefficient β_3, has a weak effect on the time shift of the field, the time shift speed is relatively low. Moreover, high odd order dispersion also affects the direction and speed of the time shift. In the third-order dispersion example, the positive and negative values correspond to the opposite directions of time shift. The larger the third-order dispersion is, the faster the time shift is. On the other hand, high even order dispersion is added into the theoretical simulation, which indicates no change in the number or position of the pulses. Therefore, the high even order dispersion does not affect the stable distribution. As a result, the drift velocity and direction of Turing patterns can be controlled by changing the magnitude of high odd dispersion. In addition, the dispersive wave of Turing patterns with high order dispersion, which represents the spectral properties of the optical field, is investigated. When the initial field in microresonators is a Gaussian pulse, frequency detuning plays a major role, and four pulses are generated in the microresonators. The field of multiple pulses experiences a time shift because of the third-order dispersion. Moreover, high order dispersion affects the spectrum, the comb spectrum is obviously modulated. The position relationship of spectrum and dispersive wave curves indicates that the zero points of the dispersive wave curves correspond to the mode number of spectral sub-

peaks. When frequency detuning is further aggravated and high order dispersion remains constant, the multi-pulse field evolves into another kind of Turing patterns that contains numerous equally spaced pulses. And the third-order dispersion can cause the time shift of the Turing patterns or multiple pulses, and the zero frequency position of the dispersive wave curves with third-order dispersion relates to the sub-peak in the spectrum. This condition means that the strongest new exciting modes with third-order dispersion have a dispersion frequency of 0. An increase in β_3 results in the augmentation of the slope of the dispersive wave curves, which means that a strong high order dispersion leads to a strong dispersive wave for high order modes of Turing patterns. However, it has almost no effect on the low order modes, the dispersive wave is nearly close to zero. Hence, high order dispersion strengthens the dispersive wave for high order modes of Turing patterns. The results of the theoretical analysis are crucial for studying Turing patterns in microresonators, whose material has a large high order dispersion.

Key words: Ultrafast optics; Microresonator; Turing patterns; High-order dispersion; Dispersive wave

OCIS Codes: 140.3430; 140.4780; 140.4780; 140.7090

Foundation item: National Natural Science Foundation of China (Nos. 52175503, 52005147), National Key Research and Development Program of China (No. 2019YFE0107400)